processes

MDPI

Article

Effect of Bone Morphogenic Protein-2-Loaded Mesoporous Strontium Substitution Calcium Silicate/Recycled Fish Gelatin 3D Cell-Laden Scaffold for Bone Tissue Engineering

Chun-Ta Yu [1], Fu-Ming Wang [1], Yen-Ting Liu [2,3], Hooi Yee Ng [2,3], Yi-Rong Jhong [4], Chih-Hung Hung [5,†] and Yi-Wen Chen [6,7,*,†]

1 Graduate Institute of Applied Science and Technology, National Taiwan University of Science and Technology, Taipei 10607, Taiwan; D10422605@ntust.edu.tw (C.-T.Y.); mccabe@mail.ntust.edu.tw (F.-M.W.)
2 School of Medicine, China Medical University, Taichung 40447, Taiwan; u102001416@cmu.edu.tw (Y.-T.L.); hooiyeen@gmail.com (H.Y.N.)
3 3D Printing Medical Research Center, China Medical University Hospital, Taichung 40447, Taiwan
4 Master Program for Biomedical Engineering, China Medical University, Taichung 40447, Taiwan; dragon40277ex@gmail.com
5 Department of Orthopedics, China Medical University Hospital, Taichung 40447, Taiwan; cmuhd10227@gmail.com
6 Graduate Institute of Biomedical Sciences, China Medical University, Taichung 40447, Taiwan
7 3D Printing Medical Research Institute, Asia University, Taichung 41354, Taiwan
* Correspondence: evinchen@gmail.com; Tel.: +886-4-2205-2121; Fax: +886-4-2475-9065
† These authors contributed equally to this work.

Received: 30 March 2020; Accepted: 17 April 2020; Published: 23 April 2020

Abstract: Bone has a complex hierarchical structure with the capability of self-regeneration. In the case of critical-sized defects, the regeneration capabilities of normal bones are severely impaired, thus causing non-union healing of bones. Therefore, bone tissue engineering has since emerged to solve problems relating to critical-sized bone defects. Amongst the many biomaterials available on the market, calcium silicate-based (CS) cements have garnered huge interest due to their versatility and good bioactivity. In the recent decade, scientists have attempted to modify or functionalize CS cement in order to enhance the bioactivity of CS. Reports have been made that the addition of mesoporous nanoparticles onto scaffolds could enhance the bone regenerative capabilities of scaffolds. For this study, the main objective was to reuse gelatin from fish wastes and use it to combine with bone morphogenetic protein (BMP)-2 and Sr-doped CS scaffolds to create a novel BMP-2-loaded, hydrogel-based mesoporous SrCS scaffold (FGSrB) and to evaluate for its composition and mechanical strength. From this study, it was shown that such a novel scaffold could be fabricated without affecting the structural properties of FGSr. In addition, it was proven that FGSrB could be used for drug delivery to allow stable localized drug release. Such modifications were found to enhance cellular proliferation, thus leading to enhanced secretion of alkaline phosphatase and calcium. The above results showed that such a modification could be used as a potential alternative for future bone tissue engineering research.

Keywords: strontium-doped calcium silicate; mesoporous material; bone morphogenetic protein; bone regeneration; cell-laden scaffold; bioprinting; recycling material

1. Introduction

Bone has a complex hierarchical structure with the capability of self-regeneration. The regenerating process of bone generally consists of three major steps which are known as the inflammatory stage, endochondral bone formation phase and lastly, the bone remodeling phase [1]. Bone remodeling is regulated simultaneously and rigorously via osteoclast resorption and osteoblast secretion [2]. The entire process is a well-orchestrated biological event which involves multiple cells and complex molecular signaling pathways. Even though bone tissues are known to have the capability to regenerate, certain undesirable medical situations such as resection of tumor invasion, infections, osteoarthritis and even genetic skeletal abnormalities can result in critical-sized bone defects [3]. Numerous studies have shown that >5 cm of human bone defects are considered to be critical-sized defects and in such cases, the normal bone regeneration process is severely impaired [4–6]. The current golden standard of treatment for bone defects is bone grafting, and such procedures are widely performed in orthopedic and maxillofacial surgery to augment bone regeneration. Of which, autologous bone grafting is the most preferred method; as such, transplants are considered as histocompatible and non-immunogenic, thus significantly reducing the chance of disease transmission and immuno-rejection. However, there are two major drawbacks with regards to autografts, which are limited availability and multiple harvesting surgeries, which could possibly lead to increased surgical risks and complications [4]. An alternative solution to autograft is allograft, but allografts carry a high risk of immunological rejection. Therefore, bone tissue engineering (BTE) has since emerged as a potential strategy for bone repair and regeneration. BTE has the ability to seed different types of cells onto three-dimensional porous scaffolds that are made up of biocompatible materials [7].

Among the numerous types of available biomaterials, ceramics are among the more prominent candidates for bone substitutes. Of which, calcium silicate (CS) is one of the more popular bioceramics due to its excellent biodegradation and osteoconduction ability as compared to the rest of the ceramics [8–10]. Recently, bone cements made up of calcium silicate received great attention from researchers as reports indicated that CS had the capability to release therapeutic ions such as Si and Ca ions [11]. Si ions were found to be excellent biological cues for induction of bone mineralization whilst the Ca ion served as a crucial factor for bone formation [12]. A previous study conducted by us further observed that CS-based materials had the ability to induce a layer of calcified bone-like apatite formation that could be used as a predictive marker for subsequent bone tissue formation [13]. In previous studies, it was shown that mesoporous molecules could be loaded onto CS and used in several biomedical applications, such as for molecule fluorescent labeling, as a drug carrier and as a genetic vector [14]. Such parameters were suggested to be superior characteristics for biomolecule loading and releasing [15]. Amongst the different types of ions such as zinc, magnesium and silicon, strontium (Sr) has received a considerable amount of attention in the field of BTE, as it was reported that Sr was able to enhance bone tissue regeneration [16,17]. Of which, it has been proven that Sr was able to simultaneously increase bone formation and decrease resorption. Furthermore, several studies have demonstrated that Sr-doped CS cements had better mechanical strength and enhanced biological properties as compared to neat CS cements. Recently, we managed to establish an effective dosage of Sr doping on CS scaffolds and it was shown that a certain amount of Sr doping was able to enhance mechanical properties of scaffolds. Furthermore, Sr was the only ion reported to correlate with increments of bone compressive stress. Therefore, Sr is widely used in orthopedic applications and was also proven to reduce the incidence of fractures in osteoporotic elderlies.

Due to technological advancements in science, we have a better understanding of the healing physiology of bone defects at a molecular level. Researchers have successfully identified a number of key molecules which have a crucial role to play in the healing process of bone defects [18]. Of these molecules, researchers largely focused on bone morphogenetic proteins (BMPs), which were known to be a potent osteoinductive factor. Studies have shown that BMP-containing scaffolds possess the ability to induce osteoblast development [19]. However, numerous studies have shown that the traditional method of depositing BMP-2 on the surface of materials was inefficient as it would lead to an immediate

burst release of BMP-2 after implantation [20]. As mentioned, the designs and architecture of the carriers or scaffolds play an important role in controlling the release of the growth factors [21].

Since the past decades, 3D printing has emerged as a novel and potential strategy for the fabrication of bioscaffolds, which has provided us with the flexibility to fabricate complex, versatile and free-form structures using different types of materials such as ceramics, polymers and hydrogels [22]. We can now fabricate customizable scaffolds with precise controls over pore size, pore morphology and porosity to provide better osteoconduction capabilities and for better control over the release of growth factors [19]. However, fused deposition modeling, known as the traditional method of 3D printing, involves high temperature, which makes it impossible to blend cells or growth factors into materials, due to cells being denatured or damaged during the printing process. However, 3D printing has since evolved and improved to allow for printing of photo-curable hydrogel, which has allowed for cell encapsulation. Of which, one of the most popular materials is gelatin methacryl (GelMa), which has the characteristic to become a stable cross-linked hydrogel under exposure to UV light [23,24]. Besides, GelMa has been proven to be able to enhance in vitro osteogenic differentiation and calcium deposition as well as enhance in vivo endochondral bone formation [25]. In this study, we will use gelatin sourced from fish collagen provided from the recycling of an unutilized resource and successive high value-added products [26]. Results from our previous studies have shown that mesoporous calcium silicate scaffolds could be loaded with BMP-2. In addition, such a modification was shown to enhance cellular activities. According to our knowledge, there were no studies combining encapsulated fish GelMA with SrCS/BMP-2 scaffolds, and thus this study was set up to test for this hypothesis.

In this study, we obtained gelatin from fish wastes and used it to combine with BMP-2-loaded SrCS (SrB) mesoporous nanoparticle. We aimed to design a novel BMP-2-loaded, hydrogel-based SrCS scaffold and to evaluate for its material composition and mechanical properties. It was reported that scaffolds with pores up to 500 by 500 μm were able to enhance bone regeneration and thus our design for this study was as such. Furthermore, the cellular bioactivity and growth factor-releasing profile should be observed in this study. After this, human Wharton jelly-derived mesenchymal stem cells (WJMSC) were laden with SrCS/fish gelatin (FGSr) and BMP-2-loaded SrCS/fish gelatin (FGSrB) bioscaffolds, whereby biocompatibility, alkaline phosphatase activity and calcium deposition were considered to determine if FGSrB could lead to enhanced bone tissue formation and regeneration.

2. Materials and Methods

2.1. Synthesis of SrCS Mesoporous Nanoparticles

The SrCS mesoporous powders were synthesized using methods established by previous reports [15,27]. Briefly, 3.3 g of cetyltrimethylammonium bromide (CTAB, Sigma-Aldrich, St. Louis, MO, USA) and 6 mL of NH_3 H_2O were mixed with double-distilled water (ddH_2O, 300 mL) and stirred for 15 min at 60 °C. Next, 15 mL of tetraethyl orthosilicate (TEOS, Sigma-Aldrich, St. Louis, MO, USA), 15.6 g of calcium nitrate (Sigma-Aldrich) and 10.6 g of strontium nitrate (Sigma-Aldrich) were added into the above solution and stirred for another 3 h. The solution was then filtrated and the precipitate was washed thrice with 1 N hydrochloric acid and ethanol, alternatively. The precipitate was placed into a 60 °C oven for 12 h and then sintered at 800 °C for 2 h at room temperature. The powder collected was characterized using small-angle X-ray diffraction (Bruker D8 SSS, Karlsruhe, Germany) and transmission electron microscopy (TEM, JEM-1400, JEOL, Tokyo, Japan).

2.2. BMP-2 Loading

BMP-2-loaded SrCS (SrB) was prepared by immersing SrCS powder in BMP-2 (MP Biomedicals, Solon, OH, USA) solution (0.5 mg/mL) for 12 h at room temperature. The SrB powder was then centrifuged at 15,000 revolutions per minute (rpm) for 15 min to remove any unloaded BMP-2. Then, the BMP-2 concentration in the supernatant was analyzed using an enzyme-linked immunosorbent

assay kit (Invitrogen, Carlsbad, CA, USA). After this, the SrB powder was washed with ddH_2O, freeze dried for 24 h and stored in a 4 °C vacuum.

2.3. FGSr and FGSrB Scaffold Fabrication

Fish skin-based gelatin methacrylate commercial bioink (GelMa-Fish, Ever Young BioDimension, Taichung, Taiwan) was used in this study. SrCS and SrB were mixed into 5% FGelMA gel and stirred for 1 h to allow uniform mixing of powder. These two groups were named FGSr and FGSrB, respectively. After this, a Pluronic® F-127 was used to print out a mold of the support using an extrusion-based 3D printer (BioX, Cellink, Gothenburg, Sweden). The respective hydrogels were then deposited into the mold and exposed to 365 nm UV light (Spot UV irradiation units, Spot Cure Series, SP11, Ushio, Japan) for 90 s. The F-127 was then removed by rinsing the hydrogels with cool distilled water.

2.4. Chemicophysical Properties Analysis

X-ray diffractometry (XRD) was used to confirm the crystallization properties of the FGSr and FGSrB scaffolds. The measurement of tensile strength of the wet specimens was conducted using the EZ-Test machine (Shimadzu, Kyoto, Japan). The test samples were fabricated into a dumb-bell shape and subsequently stretched from both ends at a rate of 1 mm/s until the sample was torn in the middle. The morphology of the scaffold before and after immersion in simulated body fluid (SBF) was investigated under a scanning electron microscope (SEM, JSM-6700F, JEOL, Tokyo, Japan).

2.5. BMP-2 Release

The drug-releasing profiles of the FGSrB scaffold were considered by immersing it in 5 mL of Dulbecco's Modified Eagle's Medium (DMEM, Invitrogen, Carlsbad, CA, USA) at 37 °C. In order to simulate the release of BMP-2 in cell culture experiments, DMEM was used as the solution for the release test, and different samples were used at each time point. The concentration of BMP-2 released from the scaffold was determined using an enzyme-linked immunosorbent assay kit (Invitrogen, Carlsbad, CA, USA) by following the manufacturer's instructions. The concentration of BMP-2 was compared to a standard curve, and a blank scaffold was used as control. All immunofluorescence readings were determined using a 96-well spectrophotometer (TECAN Infinite Pro M200, Männedorf, Switzerland).

2.6. Cell Proliferation

The human Wharton jelly mesenchymal stem cells (WJMSC) used in this study were obtained from the Bioresource Collection and Research Center, Hsin-Chu, Taiwan. WJMSCs were cultured in a commercially available mesenchymal stem cell medium (#7501, Sciencell, Carlsbad, CA, USA) to passage 4–8. To determine the cytotoxicity of the FGSr and FGSrB scaffolds, WJMSC suspensions containing 1×10^6 cells were mixed into 1 mL of FGSr or FGSrB bioink. The cell-laden FGSr or FGSrB was then printed into scaffolds and further cultured in the stem cell medium. Live/dead assay (calcein-AM and ethidium homodimer-1 stains) was used to determine indirect cytotoxicity of scaffolds. A confocal spectral microscope (Leica TCS SP8, Wetzlar, Germany) was used to observe for cellular morphology. In addition, 3-(4,5-Dimethylthiazol-2-yl)-2,5-diphenyltetrazolium bromide (MTT, Sigma-Aldrich) was used to determine the quantity of live cells in the scaffolds at different time periods.

2.7. Osteogenesis-related Protein Assay

For this study, WJMSC-laden scaffolds were cultured with a commercial osteogenesis medium (StemPro™ osteogenesis differentiation kit, Invitrogen, Carlsbad, CA, USA) for a certain duration. To determine osteogenic capabilities of the various scaffolds, the cell-laden FGSr and FGSrB scaffolds were washed thrice, treated with NP40 Cell Lysis Buffer (Invitrogen) and centrifuged for 20 min at 8000 rpm. Each sample was mixed with p-nitrophenylphosphate (pNPP, Sigma-Aldrich) in

diethanolamine buffer for 30 min. After which, 5 N NaOH was added to stop the reaction. All immunofluorescence readings were determined using a 96-well spectrophotometer (TECAN Infinite Pro M200, Männedorf, Switzerland), and all data were normalized to a standard curve obtained from a bicinchoninic acid (BCA) protein assay kit (Thermo Fisher Scientific, Waltham, MA, USA). In addition, we considered other osteogenic-related proteins by ELISA kit (Abcam, Cambridge, MA, USA), such as collagen I (Col I), osteopontin (OPN) and osteocalcin (OC).

2.8. Mineralization

The mineralized nodule formation and calcium deposition behaviors of the cell-laden FGSr and FGSrB scaffolds were analyzed after 7 and 14 days of culture. After this, the scaffolds were fixed using 4% paraformaldehyde (Sigma-Aldrich) for 15 min and further stained with 0.5% Alizarin Red S (Sigma-Aldrich) at pH 4.2 for 30 min. Subsequently, a stereomicroscope (BX53, Olympus, Tokyo, Japan) was used to observe for the morphology. Furthermore, Alizarin Red S with 20% methanol and 10% acetic acid was used to stain the scaffold for 15 min. All immunofluorescence readings were determined using a 96-well spectrophotometer (TECAN Infinite Pro M200, Männedorf, Switzerland).

2.9. Statistical Analysis

One-way variance statistical analysis was used to assess significant differences in each group, and Scheffe's multiple comparison test was used for each specimen. $p < 0.05$ was considered statistically significant. All tests were repeated 6 times independently and the average recorded.

3. Results and Discussion

3.1. Scaffold Fabrication

From our previous studies, we have demonstrated that 3D scaffolds could be modified with mesoporous nanoparticles and that such scaffolds present enhanced behaviors that could make them a potential target for bone tissue engineering application [21]. As mentioned, our previous study showed that BMP-2 could be loaded onto PDA particles and that such a modification could enhance cellular activities and subsequent bone formation. Another of our studies showed that CS could be modified with Sr, and similarly, test results showed that such a modification was able to enhance bone regeneration capabilities. In addition, a recent article published by us stated that fish GelMA could be modified with SrCS, and enhancement in cellular proliferation, differentiation and bone-related factors were shown. Therefore, for this study, we attempted to combine various materials and nanoparticles to attempt to fabricate a hybrid scaffold for bone regeneration. Firstly, we attempted to load Sr onto CS particles, followed by subsequent BMP-2 loading onto SrCS particles. Results from Figure 1A show that Sr could be loaded onto CS particles and that the SrCS nanoparticles were oval-shaped with multiple porous internal structures. Subsequently, we doped BMP-2 onto SrCS particles and attempted to fabricate the various scaffolds used in this study. Our first test was to evaluate for feasibility of printing such scaffolds. As seen from Figure 1B, FGSr and FGSrB scaffolds were fabricated successfully and it can be seen that all the scaffolds had even pores of 500 by 500 μm. The appearance and architecture of both scaffolds were smooth and intact without tears and breakage, thus indicating that the quality of printing was not influenced by the addition of BMP-2 (Figure 1B). As reported previously, the mesoporous structure served as an important role for osteoconduction and to enhance bone tissue regeneration and cellular response. According to current reports, it has been proven that bone regeneration could be improved with just a minimal pore size of a few hundred μm [28]. This study therefore attempted to fabricate scaffolds with a minimal pore size, and it was shown that it was possible to manufacture BMP-2-loaded scaffolds with 500 by 500 μm pores without any structural damage. We have previously shown successful doping of BMP.

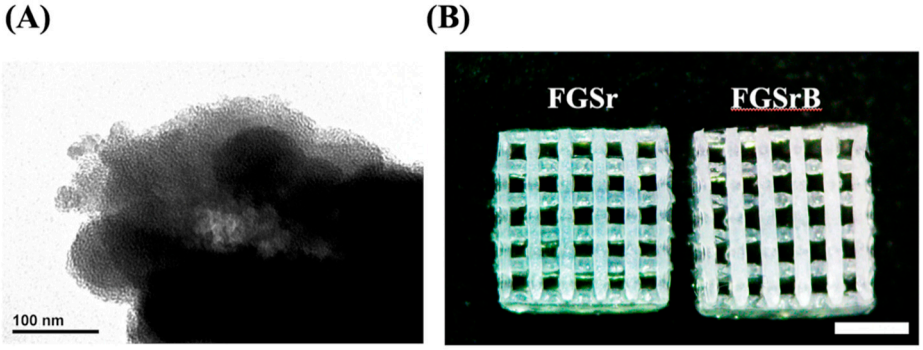

Figure 1. (**A**) TEM micrographs of mesoporous SrCS nanomaterial. (**B**) The top-view photograph of 3D-printed FGSr and FGSrB scaffolds. The scale bar is 2 mm.

Figure 2 showed the X-ray diffractometry analysis results for both the FGSr and FGSrB scaffolds. FGSrB had multiple peaks at 29.7° (C_3S), 33.3° (Sr_2SiO_4), 35° ($Ca(OH)_2$), and 32.8°, 35.2° and 40° ($SrSiO_3$) corresponded with (104), (200), (101) crystallographic planes, respectively [29], which strongly demonstrated the presence of FGSr in the compound structure; this result was consistent with that of our previous study [17]. This indicated that the addition of BMP-2 did not interrupt the original structural characteristics of FGSr, thus allowing us to retain the original beneficial properties of FGSr. Representative stress–strain curves of both FGSr and FGSrB scaffolds are shown in Figure 3. As seen, both the scaffolds exhibited almost similar mechanical properties of approximately 6.0 KPa. The results revealed that the addition of BMP-2 did not affect the original mechanical property of FGSr. Gelatin in general is too weak in mechanical properties to be used for bone tissue engineering. Therefore, it was hypothesized that the successful combination of ceramic materials with gelatin could enhance the mechanical properties of gelatin and also allow us to have beneficial properties of gelatin. At this stage, it can be seen from Figure 1B that GelMA could be combined with BMP-2-loaded SrCS particles; thus we proceeded to test for biological properties of such a scaffold. The addition of FG with SrCS gave us the capability to tune mechanical properties of the scaffold by adjusting the cross-linking parameters [30,31]. In conclusion, the addition of BMP-2 was hypothesized to provide better osteoinduction and induce osteoblast development without affecting the mechanical properties of the scaffolds, thus increasing the suitability of FGSrB scaffolds in clinical use.

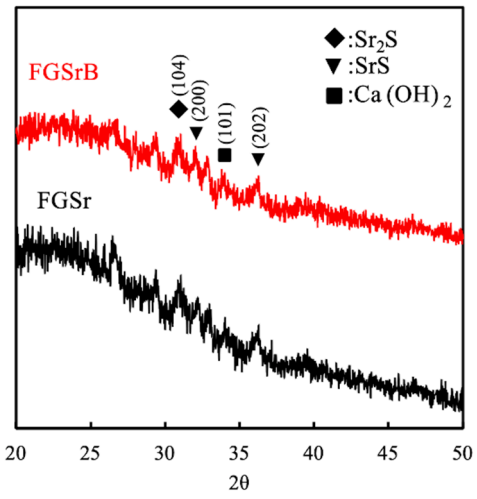

Figure 2. XRD for specimens prepared with a series of FGSr and FGSrB scaffolds.

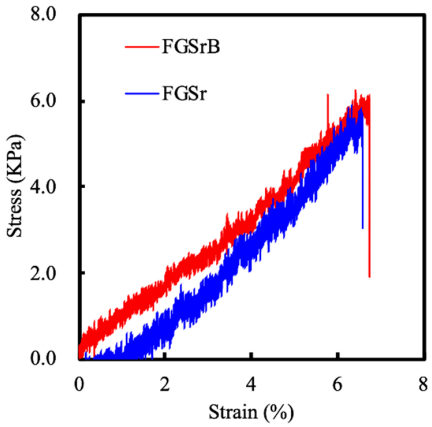

Figure 3. Tensile stress–strain curves of 3D-printed FGSr and FGSrB specimens.

Figure 4 shows the morphology and microstructures of the FGSr and FGSrB scaffolds. The FGSr and FGSrB scaffolds have irregular contour structures and many inorganic aggregates distributed evenly on the surface of the scaffold. According to literature, BMP-2 was known to enhance bone regeneration and it was hypothesized that BMP-2 works by increasing hydroxyapatite formation, thus enhancing bone formation and integration with living tissues [32]. After 3 days of immersion, SEM images showed that there were apatite aggregations on the surfaces of both scaffolds. However, it can be observed that there were more aggregations on the FGSrB scaffold as seen from the area of rough surfaces. In previous studies, we have demonstrated that FG and Sr, when applied alone, were able to increase apatite aggregations as compared to their control [33]. Thus, from this study, it can be seen that levels of apatite aggregations were increased when SrCS was modified with FG and BMP-2. In addition, the amount of apatite precipitated on the surface of bioceramics was often used as a good predictor for subsequent bone tissue formation, including cell attachment, proliferation and mineralization [34].

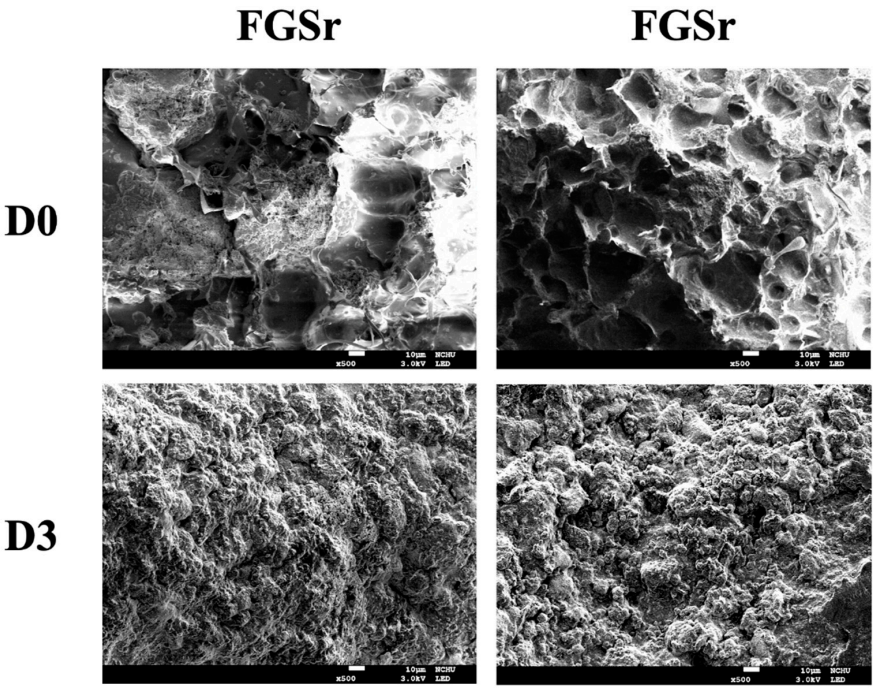

Figure 4. Microstructure images of the FGSr and FGSrB scaffolds before and after immersion in SBF. The scale bar is 10 μm.

3.2. BMP-2-Released Profile

The protein-release profiles of FGSrB scaffolds for short periods (24 h) and long periods (168 h) were analyzed to determine the drug-release potential of the scaffolds. As seen from Figure 5, it can be seen that there was a burst release of BMP-2 during the first 24 to 48 h. After this, the release of BMP-2 became attenuated and gradual, and there was release up until 168 h of immersion. The total amount of BMP-2 release over an immersion period of 168 h was 8.58 ng, and this concentration was 32.5% of the total loaded concentration. According to our experiences, we noted that it was difficult to control the steady release of BMP-2 from scaffolds; thus we always attempted to load higher concentrations to compensate for the short half-life of BMP-2 in order to allow effective bone formation. A steady release was important as a high concentration could cause various side effects, such as heterotopic bone formation, edema or inflammatory reactions [35]. In order to solve this problem, some studies have used the encapsulation of BMP-2 in micro- or nanoparticles and incorporated in the composite scaffolds [36]. Our previous results have shown that pre-loading of factors into raw materials had better sustained-release profiles as compared to direct loading of factors [19]. It was reported that scaffolds with direct loading had a steeper burst during the first 24 h as compared to pre-loading because there was an immediate desorption of factors from the surfaces of the scaffolds. Sun et al. indicated that 3D scaffolds contained mesoporous nanoparticles loaded with growth factor that enhanced stem cell proliferation and migration for in vivo treatment [37]. Therefore, we believe that the slow and sustained release of BMP-2 from the FGSrB scaffold may have the opportunity to be applied to clinical orthopedic materials in the future.

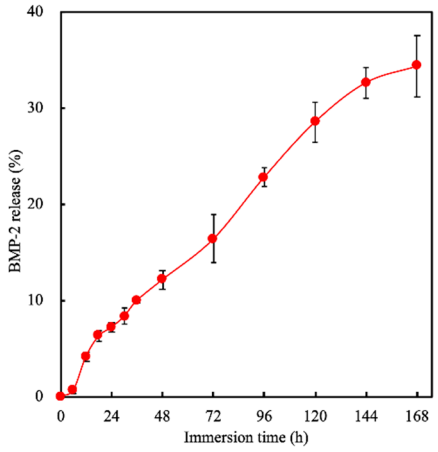

Figure 5. Bone morphogenetic protein (BMP)-2 release from FGSrB scaffold after immersion in Dulbecco's Modified Eagle's Medium (DMEM) at 37 °C for different time points. Data presented as mean ± SEM, $n = 6$ for each group.

3.3. Cell Proliferation

The level of cellular proliferation was measured using live/dead fluorescence visualization and quantifications at various time points. As can be seen in Figure 6A, the WJMSC in both the FGSr and FGSrB groups are almost alive (green staining) after being cultured for 1 day. In addition, there were more cell numbers on FGSrB as compared to FGSr. Cells on the FGSr scaffold were rather scattered whilst cells on the FGSrB scaffold almost covered the entire surface of the scaffold. From the quantification results on Figure 6B, we could note that addition of BMP-2 significantly upregulates cellular proliferation at all time points. There was approximately 1.3 to 1.5 times more cells on FGSrB scaffolds at all time points. In a previous study, we stated that enhanced initial proliferation and differentiation would lead to subsequent increased cellular bioactivities in FGSr [25]. Similarly, from this result, it can be seen that the BMP-2-loaded SrCS promoted cellular proliferation via activated BMP-2 receptor [38]. However, the clinical significance and biological functions of BMP-2 remain unknown

up until now. Studies have reported that upregulation of BMP-2 was observed in several types of cancer cell lines by using genome-wide transcriptome analysis techniques. Overexpression of BMP-2 in cancer cells led to regulation of cellular proliferation, migration and invasiveness. Nevertheless, from this study, it can be seen that BMP-2 could be included onto our biomaterial to enhance cellular proliferation [22]. It was hypothesized that the enhanced proliferation would lead to subsequent enhanced bone tissue regeneration and healing.

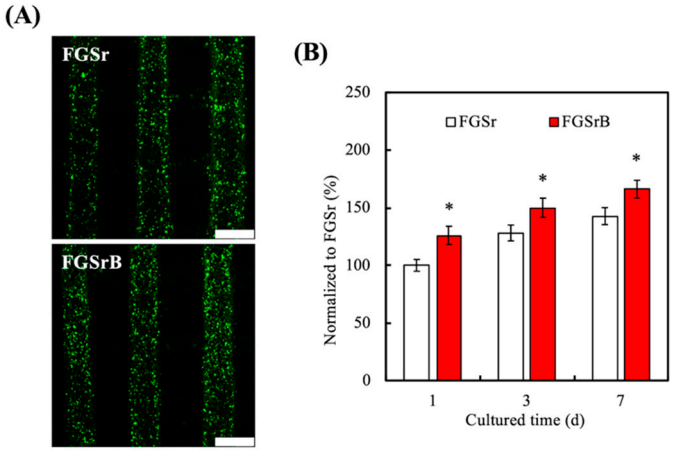

Figure 6. (**A**) The image of live/dead assay results of Wharton jelly-derived mesenchymal stem cells (WJMSC)-laden FGSr and FGSrB scaffolds for 1 day. Scale bar: 400 µm. (**B**) Cell viability of WJMSC-laden FGSr and FGSrB scaffolds for different time points Data presented as mean ± SEM, $n = 6$ for each group. "*" indicates a significant difference ($p < 0.05$) when compared to FGSr.

3.4. Osteogenesis

BMP-2 has been shown and proven to stimulate production of bone tissues. During bone formation, BMP-2 plays a fundamental role in a complicated cascade of events that involves a number of stimulatory factors and cells types. Even if BMP-2 exhibits direct action in recruiting cells to the area and stimulating cell differentiation, the natural biology of bone formation remains intact. Those growth factors are therefore thought to initiate, stimulate and increase the normal bone formation cascade. Recombinant human BMP-2 (rhBMP-2) is already available in the USA for various orthopedic uses such as tibial fractures [39]. However, current treatments using rhBMP-2 are currently rather limited as we are unable to directly inject rhBMP-2 into bone defects. rhBMP-2 has also shown to be useful in reducing pain after anterior lumbar interbody arthrodesis with degenerative lumbar disc diseases [40]. Similarly, other studies have shown that the addition of BMP-2 onto autografts or allografts were able to improve fusion rates. Therefore, the levels of osteogenic-related factors, such as Col I, ALP, OPN and OC, were quantified and shown in Figure 7. Col I is an important component of the bone extracellular matrix and it is known to be the framework and support for cells. As seen from Figure 7A, levels of Col I at 3 and 7 days of culture for FGSrB were found to be higher than FGSr. A large number of studies have pointed out that Col I was heavily involved in regulating the mechanical strength of bones, especially in determining toughness of bones. Although Col I was not found to be significantly higher in our study, this increment indicated that addition of BMP-2 induced higher secretions of Col I from cells. In addition, it was also critical to note that ALP was known as an early indicator of osteoblastic lineage and also was an important factor in the early mineralization processes associated with bone formation [41]. Thus, the levels of ALP could be used as a predictive marker for subsequent bone tissue formation. As seen from Figure 7B, the levels of ALP were significantly higher on the FGSrB scaffolds at all time points as compared to FGSr. There was an approximate 1.3 times constant increment of ALP from the FGSrB scaffolds at all time points.

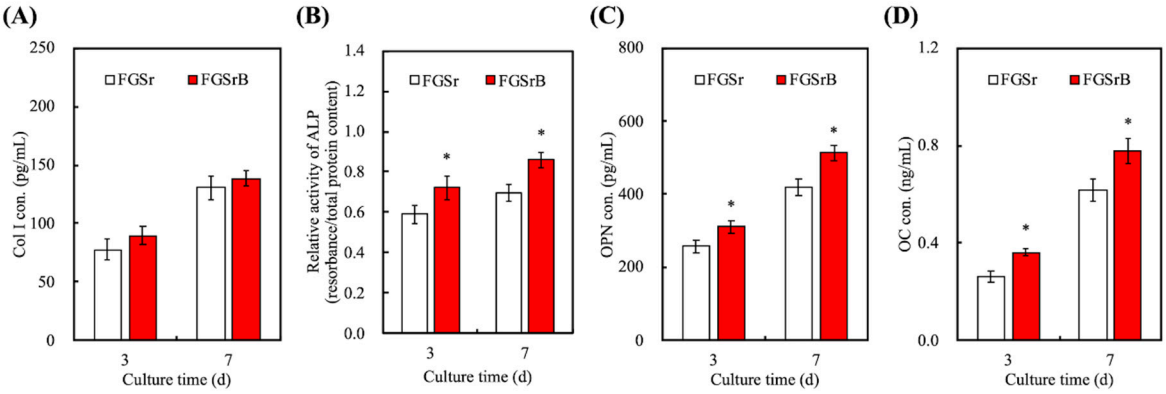

Figure 7. (**A**) Col I, (**B**) ALP, (**C**) OPN and (**D**) OC profiles of the WJMSC-laden FGSr and FGSrB scaffolds in osteogenic differentiation medium. "*" indicates a significant difference ($p < 0.05$) when compared to FGSr. Data presented as mean ± SEM, $n = 5$ for each group.

Osteopontin (OPN) is an extracellular matrix protein that is known for its function as a bridging protein. As seen from Figure 7C, FGSrB had a significantly higher amount of OPN secretions at both 3 and 7 days as compared to FGSr. After 7 days of culture, FGSrB had approximately 1.3× higher OPN levels than FGSrB at 490 versus 405 ng/mL, respectively. OC, on the other hand, is a non-collagenous protein hormone that is secreted only by osteoblasts and is known to be involved in bone formation. Similarly, FGSrB had significantly higher levels of OC on both days as compared to FGSr. These results were in good agreement with the proliferation results above in that BMP-2 was known to be an important factor in both cellular proliferation and bone tissue formation. Some studies have demonstrated that the interaction of Sr with growth factor can promote and accelerate secretion activity [42]. Zhao et al. indicated the scaffold coated with BMP-2 revealed excellent bioactivity with promoted osteogenesis differentiation of pre-osteoblast by markedly enhancing osteogenesis-related gene expression, ALP activity and calcium mineralization [43].

The osteogenic behaviors of both scaffolds were evaluated by placing cells in the presence of the osteogenesis differentiation medium [44]. The evaluation in this study was done using Alizarin Red S staining analysis and calcium quantification on both scaffolds at days 7 and 14 of culture (Figure 8). The main aim of the Alizarin Red S staining was to reveal the presence of calcium stores in the extracellular matrix of cells and in the culture medium. As seen from Figure 8A, FGSrB had a darker density of Alizarin Red S staining on both days 7 and 14 as compared to FGSr, thus indicating that there was more calcium deposition present. Furthermore, there were more white patches present on the FGSr scaffolds as compared to its counterpart. However, such visual observations tend to be rather user-biased; therefore, calcium quantification was done to augment the above results. As seen on Figure 8B, calcium quantification results showed that FGSrB had significantly higher amounts of calcium deposition as compared to FGSr. There was an approximately 1.3× higher amount of calcium deposition on FGSrB as compared to FGSr. Hence, both the results were in good agreement with each other. Such calcium depositions formed a mineralized matrix on the surface of the scaffolds which could be used as a phenotypic marker for a larger stage of osteoblastic differentiation. FGSrB had a significantly elevated amount of calcified matrix as confirmed by both the Alizarin Red S staining and the quantification results. Xie et al. explained that Sr ion directly regulated osteoblast behaviors and inhibited the function of osteoclasts with a particularly marked outcome on bone remodeling [45]. Therefore, it was demonstrated that the addition of BMP-2 was capable of enhancing bone regeneration and could be a potential candidate for bone tissue engineering [46]. BMP-2 enhanced biocompatibility by promoting cellular adhesion and proliferation, and thus led to subsequent enhanced cellular activities. Furthermore, WJMSC recruitment and bone formation occurred with BMP-2, especially with a rationally designed sequential delivery and released system.

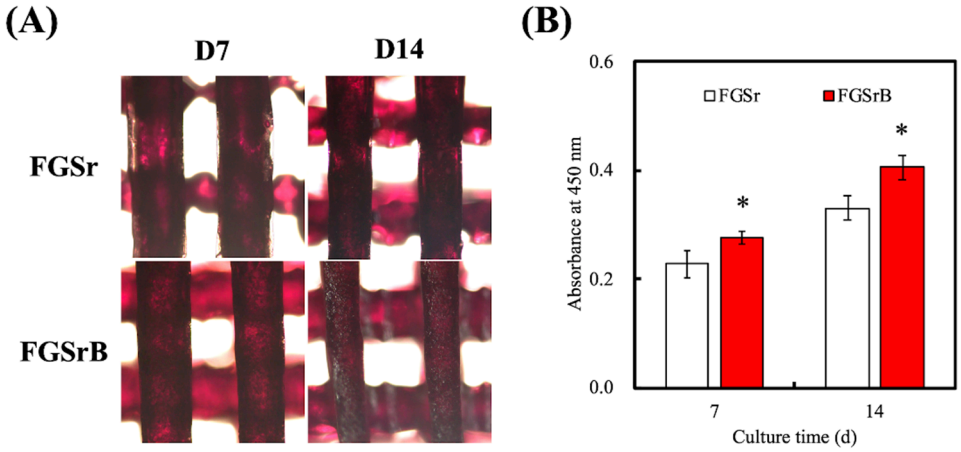

Figure 8. (**A**) Alizarin Red S staining and (**B**) quantification of calcium mineral by WJMSC-laden scaffolds. "*"indicates a significant difference ($p < 0.05$) when compared to FGSr scaffold. Data presented as mean ± SEM, $n = 5$ for each group.

4. Conclusions

In summary, the FGSr 3D scaffolds were fabricated using a biofabrication method with suitable mechanical properties and biobehaviors in which attachment, proliferation and mineralization of WJMSC were regulated on the FGSrB scaffold. In addition, the FGSrB scaffold was demonstrated to be efficient in carrier BMP-2 with the controlling release rate for WJMSC differentiation. The FGSrB scaffold demonstrated excellent functions for WJMSC, such as proliferation and osteogenesis differentiation, and effectively sustained release of BMP-2. Therefore, we think the FGSrB scaffold combined the delivery of BMP-2 and Sr ion and could trigger various signaling pathways in WJMSC. These 3D-fabricated FGSrB bioscaffolds may be a promising and potential candidate for bone tissue regeneration in the future.

Author Contributions: Data Curation, F.-M.W.; Formal Analysis, Y.-T.L.; Funding Acquisition, Y.-W.C. and C.-H.H.; Investigation, Y.-R.J.; Methodology, Y.-T.L. and H.Y.N.; Writing—Original Draft, C.-H.H. and C.-T.Y.; Writing—Review and Editing, Y.-W.C. All authors have read and agreed to the published version of the manuscript.

Funding: The authors acknowledge receipt grants from the Ministry of Science and Technology (MOST 108-2218-E-039-001 and 108-2321-B-039-041) of Taiwan and the China Medical University Hospital (DMR-109-080) of Taiwan.

Acknowledgments: Experiments and data analysis were performed in part through the use of the Medical Research Core Facilities Center, Office of Research and Development at the China Medical University. SEM imaging was assisted by Ya-Hsun Lin (MOST 108-2731-M-005-001).

Conflicts of Interest: The authors declare no conflict of interest.

References

1. Yun, B.G.; Lee, S.-H.; Jeon, J.H.; Kim, S.-W.; Jung, C.K.; Park, G.; Kim, S.Y.; Jeon, S.; Lee, M.S.; Park, S.H.; et al. Accelerated Bone Regeneration via Three-Dimensional Cell-Printed Constructs Containing Human Nasal Turbinate-Derived Stem Cells as a Clinically Applicable Therapy. *ACS Biomater. Sci. Eng.* **2019**, *5*, 6171–6185. [CrossRef]
2. Takayanagi, H. Osteoimmunology: Shared mechanisms and crosstalk between the immune and bone systems. *Nat. Rev. Immunol.* **2007**, *7*, 292–304. [CrossRef] [PubMed]
3. Cianciosi, A.; Costantini, M.; Bergamasco, S.; Testa, S.; Fornetti, E.; Jaroszewicz, J.; Baldi, J.; Latini, A.; Choińska, E.; Heljak, M.; et al. Engineering Human-Scale Artificial Bone Grafts for Treating Critical-Size Bone Defects. *ACS Appl. BioMater.* **2019**, *2*, 5077–5092. [CrossRef]

4. Li, J.J.; Dunstan, C.R.; Entezari, A.; Li, Q.; Steck, R.; Saifzadeh, S.; Sadeghpour, A.; Field, J.R.; Akey, A.; Vielreicher, M.; et al. A Novel Bone Substitute with High Bioactivity, Strength, and Porosity for Repairing Large and Load-Bearing Bone Defects. *Adv. Healthc. Mater.* **2019**, *8*, e1900641. [CrossRef]
5. Wang, W.; Nune, K.; Tan, L.; Zhang, N.; Dong, J.; Yan, J.; Misra, R.; Yang, K. Bone regeneration of hollow tubular magnesium-strontium scaffolds in critical-size segmental defects: Effect of surface coatings. *Mater. Sci. Eng. C* **2019**, *100*, 297–307. [CrossRef]
6. Wu, R.-X.; He, X.-T.; Zhu, J.-H.; Yin, Y.; Li, X.; Liu, X.; Chen, F.-M. Modulating macrophage responses to promote tissue regeneration by changing the formulation of bone extracellular matrix from filler particles to gel bioscaffolds. *Mater. Sci. Eng. C* **2019**, *101*, 330–340. [CrossRef]
7. Zhou, Z.; Cunningham, E.; Lennon, A.; McCarthy, H.; Buchanan, F.; Dunne, N. Development of three-dimensional printing polymer-ceramic scaffolds with enhanced compressive properties and tuneable resorption. *Mater. Sci. Eng. C* **2018**, *93*, 975–986. [CrossRef]
8. Chen, Y.-W.; Yeh, C.-H.; Shie, M.-Y. Stimulatory effects of the fast setting and suitable degrading Ca-Si-Mg cement on both cementogenesis and angiogenesis differentiation of human periodontal ligament cells. *J. Mater. Chem. B* **2015**, *3*, 7099–7108. [CrossRef]
9. Liu, W.-C.; Wang, H.-Y.; Chen, L.-C.; Huang, S.-W.; Wu, C.; Chung, R.-J.; Chung, R.-J. Hydroxyapatite/tricalcium silicate composites cement derived from novel two-step sol-gel process with good biocompatibility and applications as bone cement and potential coating materials. *Ceram. Int.* **2019**, *45*, 5668–5679. [CrossRef]
10. Chiu, Y.-C.; Shie, M.-Y.; Lin, Y.-H.; Lee, A.; Chen, Y.-W. Effect of Strontium Substitution on the Physicochemical Properties and Bone Regeneration Potential of 3D Printed Calcium Silicate Scaffolds. *Int. J. Mol. Sci.* **2019**, *20*, 2729. [CrossRef]
11. Kao, C.-T.; Huang, T.-H.; Chen, Y.-J.; Hung, C.-J.; Lin, C.-C.; Shie, M.-Y. Using calcium silicate to regulate the physicochemical and biological properties when using β-tricalcium phosphate as bone cement. *Mater. Sci. Eng. C* **2014**, *43*, 126–134. [CrossRef] [PubMed]
12. Shie, M.-Y.; Ding, S.-J.; Chang, H.C. The role of silicon in osteoblast-like cell proliferation and apoptosis. *Acta Biomater.* **2011**, *7*, 2604–2614. [CrossRef] [PubMed]
13. Xie, F.; Juan, I.G.; Arango-Ospina, M.; Riedel, R.; Boccaccini, A.R.; Ionescu, E. Apatite Forming Ability and Dissolution Behavior of Boron- and Calcium-Modified Silicon Oxycarbides in Comparison to Silicate Bioactive Glass. *ACS Biomater. Sci. Eng.* **2019**, *5*, 5337–5347. [CrossRef]
14. Shen, Y.-F.; Ho, C.-C.; Shie, M.-Y.; Wang, K.; Fang, H.-Y. Hinokitiol-Loaded Mesoporous Calcium Silicate Nanoparticles Induce Apoptotic Cell Death through Regulation of the Function of MDR1 in Lung Adenocarcinoma Cells. *Materials* **2016**, *9*, 306. [CrossRef] [PubMed]
15. Huang, C.-Y.; Huang, T.-H.; Kao, C.-T.; Wu, Y.-H.; Chen, W.-C.; Shie, M.-Y. Mesoporous Calcium Silicate Nanoparticles with Drug Delivery and Odontogenesis Properties. *J. Endod.* **2017**, *43*, 69–76. [CrossRef] [PubMed]
16. Ke, D.; Tarafder, S.; Vahabzadeh, S.; Bose, S. Effects of MgO, ZnO, SrO, and SiO2 in tricalcium phosphate scaffolds on in vitro gene expression and in vivo osteogenesis. *Mater. Sci. Eng. C* **2019**, *96*, 10–19. [CrossRef]
17. Huang, T.-H.; Kao, C.-T.; Shen, Y.-F.; Lin, Y.-T.; Liu, Y.-T.; Yen, S.-Y.; Ho, C.-C. Substitutions of strontium in bioactive calcium silicate bone cements stimulate osteogenic differentiation in human mesenchymal stem cells. *J. Mater. Sci. Mater. Electron.* **2019**, *30*, 68. [CrossRef]
18. Lin, Y.-H.; Chuang, T.-Y.; Chiang, W.-H.; Chen, I.-W.P.; Wang, K.; Shie, M.-Y.; Chen, Y.-W. The synergistic effects of graphene-contained 3D-printed calcium silicate/poly-ε-caprolactone scaffolds promote FGFR-induced osteogenic/angiogenic differentiation of mesenchymal stem cells. *Mater. Sci. Eng. C* **2019**, *104*, 109887. [CrossRef]
19. Huang, K.-H.; Lin, Y.-H.; Shie, M.-Y.; Lin, C.-P. Effects of bone morphogenic protein-2 loaded on the 3D-printed MesoCS scaffolds. *J. Formos. Med. Assoc.* **2018**, *117*, 879–887. [CrossRef]
20. Chen, Y.W.; Chen, C.C.; Ng, H.Y.; Lou, C.W.; Chen, Y.S.; Shie, M.Y. Additive Manufacturing of Nerve Decellularized Extracellular Matrix-Contained Polyurethane Conduits for Peripheral Nerve Regeneration. *Polymers* **2019**, *11*, 1612. [CrossRef]
21. Huang, K.-H.; Chen, Y.-W.; Wang, C.-Y.; Lin, Y.-H.; Wu, Y.-H.A.; Shie, M.-Y.; Lin, C.-P. Enhanced Capability of Bone Morphogenetic Protein 2–loaded Mesoporous Calcium Silicate Scaffolds to Induce Odontogenic Differentiation of Human Dental Pulp Cells. *J. Endod.* **2018**, *44*, 1677–1685. [CrossRef] [PubMed]

22. Chen, Y.-W.; Shen, Y.-F.; Ho, C.-C.; Yu, J.; Wu, Y.-H.A.; Wang, K.; Shih, C.-T.; Shie, M.-Y. Osteogenic and angiogenic potentials of the cell-laden hydrogel/mussel-inspired calcium silicate complex hierarchical porous scaffold fabricated by 3D bioprinting. *Mater. Sci. Eng. C* **2018**, *91*, 679–687. [CrossRef] [PubMed]
23. Xiao, W.; Li, J.; Qu, X.; Wang, L.; Tan, Y.; Li, K.; Li, H.; Yue, X.; Li, B.; Liao, X. Cell-laden interpenetrating network hydrogels formed from methacrylated gelatin and silk fibroin via a combination of sonication and photocrosslinking approaches. *Mater. Sci. Eng. C* **2019**, *99*, 57–67. [CrossRef]
24. Shie, M.-Y.; Shen, Y.-F.; Astuti, S.D.; Lee, A.; Lin, S.-H.; Dwijaksara, N.; Chen, Y.-W. Review of Polymeric Materials in 4D Printing Biomedical Applications. *Polymers* **2019**, *11*, 1864. [CrossRef]
25. Yu, C.-T.; Wang, F.-M.; Liu, Y.-T.; Lee, A.; Lin, T.-L.; Chen, Y.-W. Enhanced Proliferation and Differentiation of Human Mesenchymal Stem Cell-laden Recycled Fish Gelatin/Strontium Substitution Calcium Silicate 3D Scaffolds. *Appl. Sci.* **2020**, *10*, 2168. [CrossRef]
26. Dong, Y.; Chen, H.; Qiao, P.; Liu, Z. Development and Properties of Fish Gelatin/Oxidized Starch Double Network Film Catalyzed by Thermal Treatment and Schiff' Base Reaction. *Polymers* **2019**, *11*, 2065. [CrossRef]
27. Lin, W.-H.; Yu, J.; Chen, G.; Tsai, W.-B. Fabrication of multi-biofunctional gelatin-based electrospun fibrous scaffolds for enhancement of osteogenesis of mesenchymal stem cells. *Colloids Surf. B Biointerfaces* **2016**, *138*, 26–31. [CrossRef]
28. Zheng, D.; Yang, H.; Yu, F.; Zhang, B.; Cui, H. Effect of Graphene Oxide on the Crystallization of Calcium Carbonate by C3S Carbonation. *Materials.* **2019**, *12*, 2045. [CrossRef]
29. Zhao, D.; Huang, J.; Zhong, Y.; Li, K.; Zhang, L.; Cai, J. High-Strength and High-Toughness Double-Cross-Linked Cellulose Hydrogels: A New Strategy Using Sequential Chemical and Physical Cross-Linking. *Adv. Funct. Mater.* **2016**, *26*, 6279–6287. [CrossRef]
30. Rizwan, M.; Peh, G.; Ang, H.-P.; Lwin, N.C.; Adnan, K.; Mehta, J.S.; Tan, W.S.; Yim, E.K. Sequentially-crosslinked bioactive hydrogels as nano-patterned substrates with customizable stiffness and degradation for corneal tissue engineering applications. *Biomaterials* **2017**, *120*, 139–154. [CrossRef]
31. Kokkinos, P.A.; Koutsoukos, P.G.; Deligianni, D.D. Detachment strength of human osteoblasts cultured on hydroxyapatite with various surface roughness. Contribution of integrin subunits. *J. Mater. Sci. Mater. Electron.* **2012**, *23*, 1489–1498. [CrossRef]
32. Su, T.-R.; Huang, T.-H.; Kao, C.-T.; Ng, H.; Chiu, Y.-C.; Hsu, T.-T. The Calcium Channel Affect Osteogenic Differentiation of Mesenchymal Stem Cells on Strontium-Substituted Calcium Silicate/Poly-ε-Caprolactone Scaffold. *Processes* **2020**, *8*, 198. [CrossRef]
33. Cheng, Y.-L.; Chen, Y.-W.; Wang, K.; Shie, M.-Y. Enhanced adhesion and differentiation of human mesenchymal stem cell inside apatite-mineralized/poly(dopamine)-coated poly(ε-caprolactone) scaffolds by stereolithography. *J. Mater. Chem. B* **2016**, *4*, 6307–6315. [CrossRef] [PubMed]
34. Tannoury, C.; An, H.S. Complications with the use of bone morphogenetic protein 2 (BMP-2) in spine surgery. *Spine J.* **2014**, *14*, 552–559. [CrossRef] [PubMed]
35. Tan, J.; Zhang, M.; Hai, Z.; Wu, C.; Lin, J.; Kuang, W.; Tang, H.; Huang, Y.; Chen, X.; Liang, G. Sustained Release of Two Bioactive Factors from Supramolecular Hydrogel Promotes Periodontal Bone Regeneration. *ACS Nano* **2019**, *13*, 5616–5622. [CrossRef] [PubMed]
36. Sun, Y.; Han, X.; Wang, X.; Zhu, B.; Li, B.; Chen, Z.; Ma, G.; Wan, M. Sustained Release of IGF-1 by 3D Mesoporous Scaffolds Promoting Cardiac Stem Cell Migration and Proliferation. *Cell. Physiol. Biochem.* **2018**, *49*, 2358–2370. [CrossRef] [PubMed]
37. Yang, F.; Yang, D.; Tu, J.; Zheng, Q.; Cai, L.; Wang, L. Strontium Enhances Osteogenic Differentiation of Mesenchymal Stem Cells and In Vivo Bone Formation by Activating Wnt/Catenin Signaling. *Stem Cells* **2011**, *29*, 981–991. [CrossRef]
38. Wang, J.; Li, D.; Li, T.; Ding, J.; Liu, J.; Li, B.; Chen, X. Gelatin Tight-Coated Poly(lactide-co-glycolide) Scaffold Incorporating rhBMP-2 for Bone Tissue Engineering. *Materials* **2015**, *8*, 1009–1026. [CrossRef]
39. Kumar, P.S.; Hashimi, S.M.; Saifzadeh, S.; Ivanovski, S.; Vaquette, C. Additively manufactured biphasic construct loaded with BMP-2 for vertical bone regeneration: A pilot study in rabbit. *Mater. Sci. Eng. C* **2018**, *92*, 554–564. [CrossRef]
40. Wu, C.; Zhou, Y.; Lin, C.; Chang, J.; Xiao, Y. Strontium-containing mesoporous bioactive glass scaffolds with improved osteogenic/cementogenic differentiation of periodontal ligament cells for periodontal tissue engineering. *Acta Biomater.* **2012**, *8*, 3805–3815. [CrossRef]

41. Yan, S.; Feng, L.; Zhu, Q.; Yang, W.; Lan, Y.; Li, D.; Liu, Y.; Xue, W.; Guo, R.; Wu, G. Controlled Release of BMP-2 from a Heparin-Conjugated Strontium-Substituted Nanohydroxyapatite/Silk Fibroin Scaffold for Bone Regeneration. *ACS Biomater. Sci. Eng.* **2018**, *4*, 3291–3303. [CrossRef]
42. Zhao, X.; Han, Y.; Li, J.; Cai, B.; Gao, H.; Feng, W.; Li, S.; Liu, J.; Li, D. BMP-2 immobilized PLGA/hydroxyapatite fibrous scaffold via polydopamine stimulates osteoblast growth. *Mater. Sci. Eng. C* **2017**, *78*, 658–666. [CrossRef] [PubMed]
43. Kazemi, M.; Dehghan, M.M.; Azami, M. Biological evaluation of porous nanocomposite scaffolds based on strontium substituted β-TCP and bioactive glass: An in vitro and in vivo study. *Mater. Sci. Eng. C* **2019**, *105*, 110071. [CrossRef]
44. Xie, H.; Gu, Z.; He, Y.; Xu, J.; Xu, C.; Li, L.; Ye, Q. Microenvironment construction of strontium-calcium-based biomaterials for bone tissue regeneration: The equilibrium effect of calcium to strontium. *J. Mater. Chem. B* **2018**, *6*, 2332–2339. [CrossRef] [PubMed]
45. Kuttappan, S.; Jo, J.-I.; Sabu, C.K.; Menon, D.; Tabata, Y.; Nair, M.B. Bioinspired nanocomposite fibrous scaffold mediated delivery of ONO-1301 and BMP2 enhance bone regeneration in critical sized defect. *Mater. Sci. Eng. C* **2019**, *110*, 110591. [CrossRef]
46. Mandakhbayar, N.; El-Fiqi, A.; Lee, J.-H.; Kim, H.-W. Evaluation of Strontium-Doped Nanobioactive Glass Cement for Dentin–Pulp Complex Regeneration Therapy. *ACS Biomater. Sci. Eng.* **2019**, *5*, 6117–6126. [CrossRef]